J. ISSS Vol. **2** No. 1, pp. 10-19, March 2013.
REGULAR PAPER

Digital Microfluidics and its Integration with a Fluidic Microreactor

Paresh Kumar and Enakshi Bhattacharya[1]
Microelectronics and MEMS Laboratory,
Department of Electrical Engineering,
IIT Madras, Chennai-600036, India
Corresponding author: enakshi@ee.iitm.ac.in[1];

Keywords:
DMF,
Bulk Micromachining,
Integration

Abstract

We present the steps to fabricate a Digital Microfluidics (DMF) platform for handling fluidic sample delivery. This is followed by the integration of the DMF chip with a microreactor that is an Electrolyte Insulator Semiconductor Capacitor (EISCAP) biosensor. DMF is used for handling basic fluidic operations like droplet transportation, and splitting and dispensing smaller droplets from a reservoir. All the droplet operations on DI water droplets mentioned above are possible with AC actuation at ~35 V_{rms} but this result in electrolysis on the transportation of an electrolyte droplet. DC actuation is used to solve the problem of electrolysis and to transport the electrolyte droplets. Interdigitated electrode geometry improves the device performance. The DMF substrate is used to deliver fluidic samples via a through hole in the DMF wafer to a bulk micromachined EISCAP biosensor bonded to the DMF wafer. The dimension of the through hole and the extent of its coverage with the control electrode are optimized for the successful delivery of the fluidic samples to the bonded biosensor below. The devices are tested by delivering droplets of electrolyte to the bonded reactor below. Capacitance-Voltage (C-V) measurement done on the integrated device confirms the successful delivery of the electrolyte to the microreactor. This integration technique can manipulate fluid handling work on the DMF substrate without compromising the functionality of the fluidic reactor.

1. Introduction

DMF is a relatively new technology which has brought the digital revolution to the field of microfluidics and is regarded as a second generation lab-on-a-chip technology. In DMF, a liquid is manipulated in the form of individual droplets over an array of electrodes. The electrodes are embedded underneath a dielectric layer. These electrodes can be actuated in a sequential manner to move the droplet [Pollack *et al*, 2000]. DMF can perform all basic droplet-related operations like dispensing smaller droplets from on-chip reservoirs, transportation, splitting and merging on the same platform [Cho *et al*, 2003]. This revolutionary platform to manipulate individual droplets with an electric field does not need any pumps, valves or channels; hence it offers simplicity in configuration and fabrication. In addition, it offers scalable architecture and dynamic reconfigurability along with several other advantages which make DMF a suitable platform to develop lab-on-a-chip applications [Fair, 2007].

Of the different theories put forward to explain the movement of the droplet in DMF devices, one of them proposes the electrical modification of the surface tension changing the contact angle of the droplet on a hydrophobic surface as the principal reason behind droplet transportation [Pollack *et al*, 2000 and Cho *et al*, 2003]. This spreading of the liquid droplet on a solid surface upon applying potential is also known as Electrowetting on Dielectric (EWOD) [Mugele and Baret, 2005]. An alternative explanation comes from the electromechanical interpretation which considers the changes in the contact angle and the transportation of small volumes of liquid by a non-uniform electric field as distinct observables [Jones, 2005].

In this paper, we first present the development of a DMF platform for handling fluidic samples including the optimization of process steps and the driving circuit. Problems related with DMF like electrolysis, dielectric charging and their potential solutions have been discussed. Despite having several biological and chemical applications [Abdelgawad and Wheeler, 2009], the integration of the DMF device with fluidic reactors is not well explored. Here, we present the processing technique for the integration of the DMF device with a fluidic microreactor, in particular, an Electrolyte Insulator Semiconductor Capacitor (EISCAP) biosensor which can sense changes in the pH of the electrolyte; which are manifested as a shift in the capacitance voltage (CV) characteristics [Veeramani *et al*, 2013] . The integrated device reduces the problem of evaporation and can hold the liquid inside the microreactor for more than 30 minutes. The integrated device is tested with an electrolyte and the measurement of CV characteristics confirms the delivery of the electrolyte to the microreactor in the bonded wafer below. The optimization of different structures for the reliable delivery of the droplet to the microreactor and the associated problems are discussed.

2. Experimental Details

2.1 Fabrication of the DMF Device

A standard two plate DMF device is fabricated on a 500 µm thick Borofloat glass wafer. The wafers are first immersed in a boiling Trichloroethylene (TCE) solution followed by boiling acetone for two minutes each. This is followed by a thorough rinsing in running DI water of resistivity 18.2 MΩcm and blown dry in N_2. A thin layer (~180 nm) of Cr is coated on the wafer and patterned to realize the electrode array. The dimension of control electrodes are 2.6 x 2.6 mm^2 with a 30 µm gap between them. Different geometries of the electrodes have been investigated. This is followed by the deposition of a 420 nm thick layer of silicon nitride (SiN) using PECVD. The SiN deposition is carried out at 350°C, 500m Torr, and 50 W by passing Silane (20sccm) and Ammonia (20sccm) with Nitrogen (200sccm). After the silicon nitride deposition, the device is patterned to access the contact pads using standard photolithography techniques. A thin layer (~ 100 nm) of Teflon is spin-coated at 2000 rpm for 60 sec on top of the nitride layer and followed by a 10 minute post-baking on a hot plate at 160°C. The Teflon solution is prepared by mixing Teflon® AF1600 (Dupont) with Fluorinert FC-40 (Sigma Aldrich) in 1% w/w (mass/mass) concentration. This makes the top surface of the device hydrophobic, reduces the solid-liquid interaction, and helps in the smooth motion of the droplet.

An Indium Tin Oxide (ITO) coated glass plate (Delta Technologies Ltd., Stillwater, MN, USA) is used as the top plate, this act as a continuous base and has been made hydrophobic by Teflon coating. Two pieces of double-sided Scotch tape with a thickness of ~ 200 µm are used as spacers between the DMF substrate and the top plate. The plates are coupled after dispensing the droplet of DI water or electrolyte from a pipette onto one of the control electrodes. A cross sectional view of the fabricated device is shown in Figure 1.

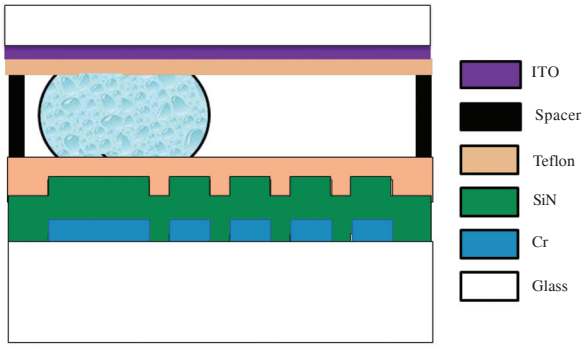

Fig. 1 Cross sectional view of the two plate DMF device

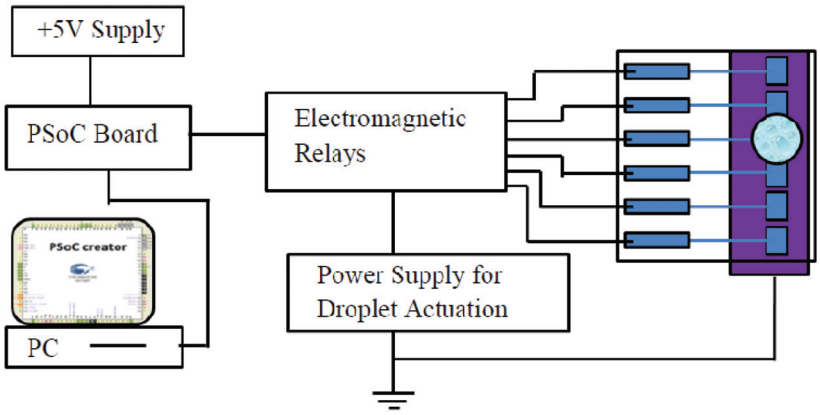

Fig. 2 Block diagram of the droplet driving system.

2.2 Driving System

Figure 2 shows a block diagram of the driving system to manipulate droplets on the DMF device. The driving system consists of a 'Programmable System on Chip' (PSoC®, Cypress semiconductor), electromagnetic relays, a dc power supply and an auto transformer to provide ac actuation potential with a fixed frequency of 50 Hz. The voltage source (ac or dc) is connected to the DMF control electrodes via relays. The PSoC is programmed to generate signals of finite duration to switch the state of relay from 'normally open' to 'close' and activate the connecting electrode. A simple code describing the on and off time for the relays is written in C language in the PSoC creator 1.0 software and is transferred to the PSoC board via the USB-JTAG adapter. To access the contact pads of the DMF device for the driving system, the DMF device is inserted into a multi-pin connector (Elcom, Single Sided Edge Connector, EC-16G). Figure 3 shows a picture of the fabricated DMF device which is fitted into the connector. The contact pads of the DMF device are laid out in the mask to match the size of the connector pins.

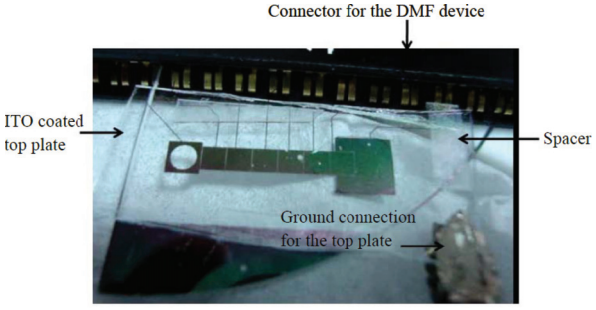

Fig. 3 Photograph of the fabricated two plate DMF device (contact pads are inserted into the connector)

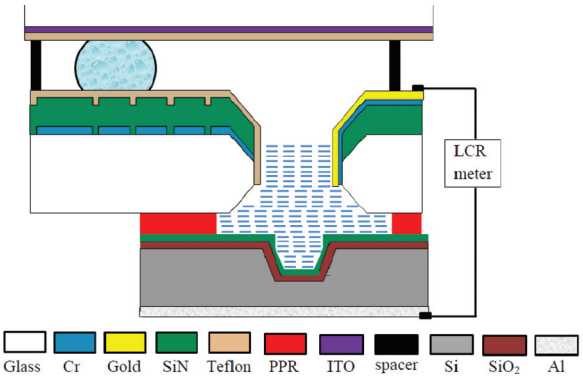

Fig. 4 Cross sectional view of the integrated device

2.3 Integration of the DMF substrate with the EISCAP

A schematic cross section of the integrated DMF-EISCAP chip fabricated is shown in Figure 4. For integration, a double side polished 500 µm thick, 4", Borofloat glass wafer is used as the substrate. Figure 5 shows the schematics of the cross section and top view of the device at every process step. First, through holes in the wafer are realized by a bulk micromachining technique. After cleaning, the wafers are coated with a thin layer of Cr (50nm)/Au(100nm) on both sides by electron beam evaporation. This is followed by gold electroplating with 0.35 mA/cm^2 current density for 50 minutes to get a thick gold layer of about 1.3 µm which acts as a mask against Hydrofluoric acid (HF) to etch the through hole (Figure 5a). The electroplated wafers are patterned on both sides using standard lithography techniques with back side alignment (BSA). Double-sided processing of the wafer is necessary to reduce the through hole etching time. SPR-220 photo-resist (PR) is used to get a thick layer of photo-resist which acts as a mask for the selective removal of the Cr/Au layer

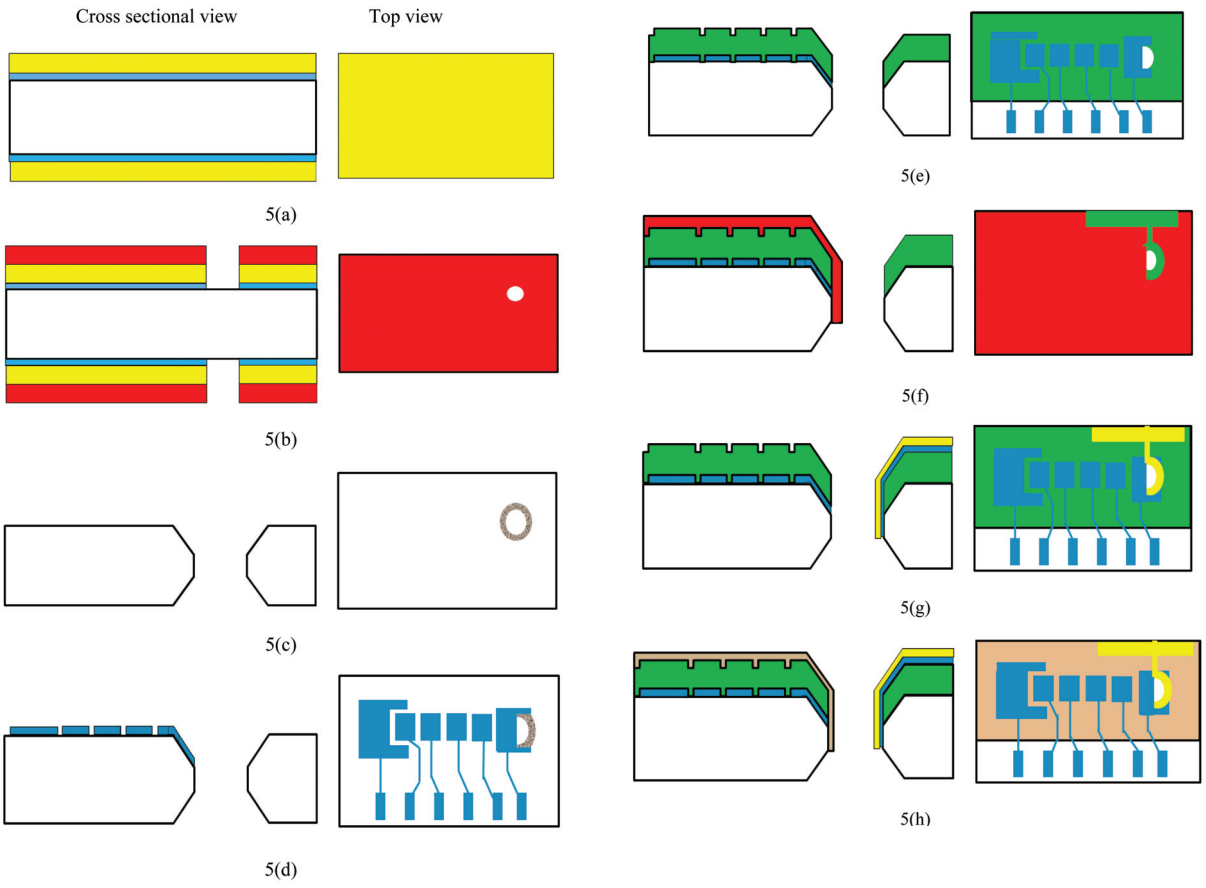

Fig. 5 Cross sectional and top views of the device: (a) after Cr/Au coating and electroplating, (b) after patterning with BSA, (c) after through hole etching, (d) after patterning of control electrodes, (e) after PECVD SiN deposition and patterning, (f) after PPR coating and developing for lift off, (g) After lift-off, (h) after Teflon coating

(Figure 5b) and also, for some time, during the through hole etching. The etching of glass is carried out to realize a through hole of diameter 1.3 mm, using 48% HF acid for 42 minutes (Figure 5c). For the control electrodes, an 180 nm thick layer of Cr is coated on the wafer and patterned to realize the electrode array (Figure 5d). The dimensions of the control electrodes and reservoir are the same as mentioned in section 3.1. Two different structures have been realized by aligning the last electrode with the through hole. In the first case, 5% of the through hole is covered with the last electrode. In the second case, 50% of the through hole is covered with the last electrode.

After the patterning of the control electrodes, 420 nm of PECVD silicon nitride (SiN) is deposited, which acts as an insulator between the droplet and the control electrodes (Figure 5e). To accommodate the electrical measurements with the electrolyte in the microreactor, a gold electrode layer is patterned using a standard lift-off process (Figure 5f and 5g) along the side wall slope of the through hole. The nitride layer is coated with a thin (~ 100 nm) hydrophobic layer of Teflon AF 1600 (Figure 5h) using the procedure described in section 3.1. Following the Teflon coating, the DMF substrate is bonded to the wafer with the EISCAP microreactor using photoresist as an adhesive. The integrated DMF platform is then pre-baked (80 °C) for 5 minutes and later post-baked (120° C) for 10 minutes to harden the PPR. The hardened PPR does not react with the electrolyte. Finally, the bottom DMF substrate is attached to the hydrophobic top plate using spacers (two pieces of double sided tape), after dispensing the electrolyte droplets from a pipette onto the control electrodes. The electrolyte is delivered by the DMF to the EISCAP biosensor via the through hole and capacitance-voltage (C-V) measurements are carried out using an LCR meter (Agilent E4980A).

3. Results and Discussions

3.1 Testing of the DMF Device

The devices are tested with droplets of DI water and the conducting electrolyte. The electrolyte is a mixture of 0.5 M KCl with a 50 mM phosphate buffer solution (PBS). An auto transformer with a fixed frequency of 50 Hz and a dc power supply are used to provide ac or dc actuation, respectively. The movements of the droplets are captured using a digital camera.

3.1.1 Effect of ac actuation

A 1.2 µl droplet of DI water is dispensed by a micropipette onto the control electrode and the circuit is completed by placing the top plate on the spacers. This squeezes the droplet over the entire electrode and the droplet meniscus makes a small overlap with the next electrode. The droplet movement is initiated at the lowest applied voltage of 21 V_{rms}. At this voltage, the droplet movement is too slow to make an overlap with the next electrode, after covering the biased electrode. The reliable transport of the water droplets over a series of five electrodes at ~2.6 mm s^{-1} is achieved with ~25.5 V_{rms}. The droplet speed increases to ~26 mm s^{-1} by increasing the actuation potential to 39 V_{rms}. The duration for the activation of each electrode is controlled using the PSoC board and the electromagnetic relays.

3.1.1.1 Transportation Statistics

The time required for droplet transportation is reduced with the applied voltage. Figure 6 shows typical actuation characteristics for the droplet over an electrode. To measure the actuation timings, a droplet is placed on the control electrode. The control electrode is then actuated to spread the droplet over its entire surface and to make about a 10% overlap with the next electrode (denoted by E1), as shown in Figure 6 (a). The droplet is said to be transported reliably when it moves over a series of three electrodes denoted by E1, E2 and E3 (Figure 6a), in the least possible actuation time. The actuation timing strategies play an important role in the reliable transport of the droplet from one electrode to the next. Figures 6(b) and 6(c) show different timing strategies which are denoted by On_On and On_Off_On respectively. The effect

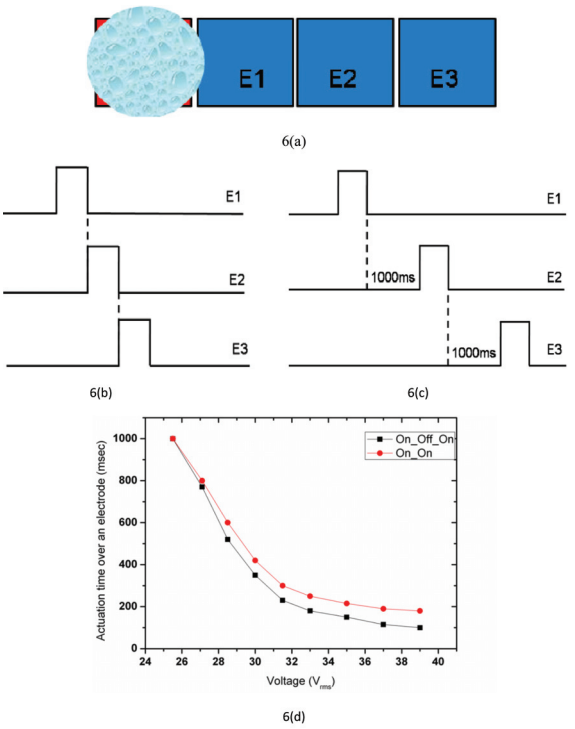

Fig. 6 Effect of actuation timings on the DMF device performance: (a) **experimental measurement set-up,** (b) **On_On timing strategy,** (c) **On_Off_On timing strategy and** (d) **Typical actuation characteristics of the droplet over a DMF electrode**

of these timings on droplet transportation can be observed in Figure 6(d).

The On_Off_On timing strategy can move the droplet more reliably and repeatedly, than the On_On timings. The effect of the timing strategies becomes more significant when the actuation time is less than 600 ms. At this high speed, the On_Off_On strategy gives a sufficient interval for the droplet to overlap with the next electrode during the Off time. The Off timings have been kept at 1000 ms in our experiments. The actuation time for the On_Off_On timing strategy denoted in Figure 6(d) excludes the Off time.

3.1.1.2 Cutting and Dispensing

In addition to droplet transportation, the cutting of a DI water droplet and the creation of smaller droplets from the reservoir are demonstrated. Droplet division is successfully performed at 35 V_{rms}. Figure 7 presents the sequential frames of the division operation. In the beginning, the droplet occupies the entire middle electrode and makes a small overlap with the neighboring electrodes. Upon

actuating both the neighboring electrodes, the droplet is elongated in the longitudinal direction. Meanwhile, the middle electrode is kept floating. This contracts the meniscus on it due to its hydrophobic surface and in order to keep the total volume of the droplet constant. Finally, the neck is pinched off and cutting is achieved.

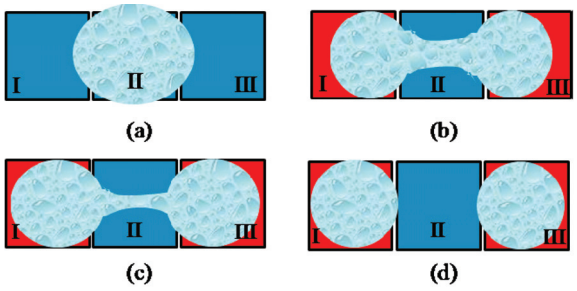

Fig. 7 Schematics of the sequential frames for cutting of a 1.2 µ– DI water droplet

The creation of small droplets from the reservoir is demonstrated at an applied voltage of 35 V_{rms}. In the beginning, a liquid column is formed by sequentially activating the first three electrodes. When the front end of the liquid column reaches the third electrode, both the third and the reservoir electrode are activated simultaneously. Consequently, droplet necking occurs on the second electrode, a small droplet is created on the third electrode and the liquid column is pulled back to the reservoir (Figure 8).

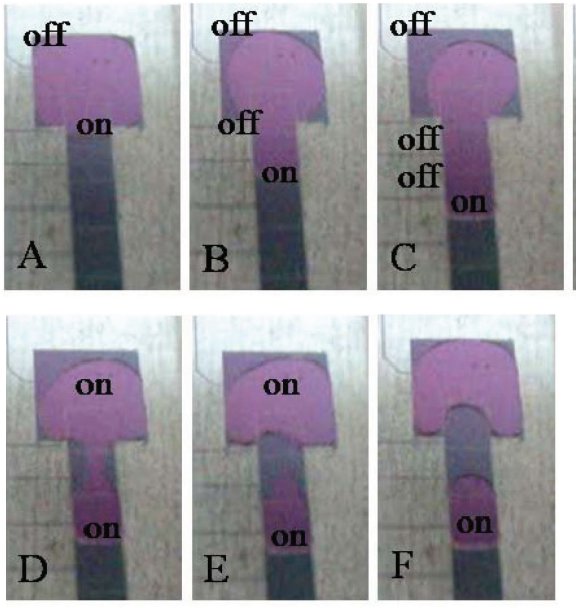

Fig. 8 Sequential frames showing creation of a droplet from reservoir with ~35 V_{rms}. The 'on' and 'off' denote to activated and floating electrode respectively.

3.1.1.3 Transportation of the Electrolyte Droplet

Though the devices are able to move the droplet with 30 V_{rms}, they suffer from the problem of bubble formation in the droplet possibly due to the onset of 'electrolysis' soon after applying the potential. The small bubbles in Figure 9 indicate the flow of current through the insulating layer while transporting the droplet. This damages the device permanently and can be attributed to the poor dielectric characteristics of the PECVD silicon nitride layer. This is more apparent during the actuation of conductive liquids because all of the applied voltage is dropped across the dielectric layer. This, in turn, causes a large displacement current to flow through the silicon nitride layer and eventually leads to electrolysis. This is in contrast with the normal trend where ac actuation is always preferred for droplet movement to avoid dielectric charging. But most of these studies use either a thicker dielectric layer with air as a medium [Chatterjee *et al*, 2006] or a high quality pin-hole free thinner dielectric layer with oil as a medium [Chang *et al*, 2006] to achieve a better performance.

3.1.2 Effect of DC Actuation

The problem of electrolysis during the transportation of an electrolyte solution is mitigated using dc actuation potential. The droplet (both DI water and electrolyte) movement is initiated at 30 V but the droplet speed is too low to spread over the entire actuated electrode surface and to overlap with the next electrode. Higher operating voltages (>37 V) with multiple actuations are required for a small overlap of the droplet's contact line with the next electrode. We think this problem is due to the charging of the dielectric layer. This is supported

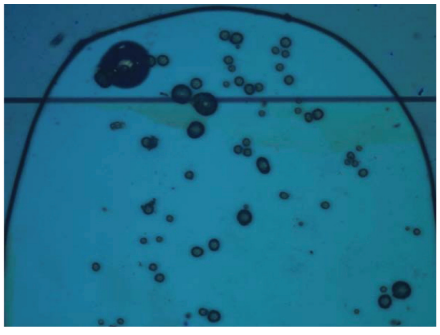

Fig. 9 Electrolysis during transportation of the electrolyte droplet on SiN coated DMF device under ac actuation

by a closer look at the contact line of the droplet with 50X zoom using a Nikon Microscope (Nikon LV145A).

Figure 10 shows the picture of the contact line of the droplet during transportation from one electrode to the next using a dc (37 V) and ac (30 V_{rms}) actuation potential. The 'on' electrode represents the activated electrode where the droplet is moving and the 'off' electrode denotes the next electrode where the droplet is going to move after making a small overlap. As shown in Figure 10 (a), under dc actuation, the droplet first covers the entire actuated electrode surface and upon further actuation, the droplet tries to adhere to the actuated electrode boundary, without making any overlap to the next ('off') electrode. A small overlap of the droplet front meniscus with the next electrode (currently 'off') is necessary to provide sufficient electromechanical force to move the droplet. This overlap is achieved upon applying multiple actuations to the 'on' electrode.

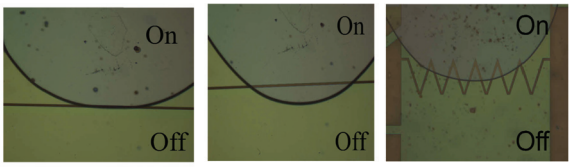

Fig. 10 Top view of the droplet contact line while moving from one electrode ('on') to next ('off'). (a) Under dc actuation (b) Under ac actuation and (c) Under dc actuation with interdigitated electrode shape

Using multiple actuations reduces the fidelity between the driving time specified by the droplet manipulation system (Figure 2) and the droplet transportation from one electrode to the next electrode as the droplet sticks to the actuated electrode boundary. Due to this unpredictability of the overlap, the droplet driving system cannot be used to provide the driving signals to transport the droplets, under dc actuation. This problem is not observed with ac actuation because in this case, the dielectric layer does not get charged. The droplet meniscus, under ac actuation, immediately makes an overlap with the next electrode after covering the actuated electrode as shown in Figure 10(b).

3.2 Interdigitated Electrode Structure

The problem of overlapping with the next electrode during transportation can be solved by using an interdigitated electrode shape [Pollack *et al*, 2002]. DMF devices with interdigitated triangular fingers are fabricated with the same process flow described in section 3.1. The devices with a zigzag edge pattern are able to perform essential droplet operations on both the DI water and the electrolyte droplet. When compared with the flat edge electrode, the use of a dc actuation potential does not hamper the smooth motion of the droplet. As shown in Figure 10(c), upon applying the dc actuation potential to the 'on' electrode, the triangular fingers at the edge of the electrode take care of the required overlap to the next electrode. Due to this overlap, the droplet moves very quickly over the next electrode when it is actuated. It also requires a lower operating voltage of 33 V to transport an electrolyte droplet over a series of five electrodes without the need of multiple actuations as compared to a device with a flat-edged electrode. Due to the larger overlap for the interdigitated electrodes, the voltage required for actuation is less than that in planar electrodes. This, and the faster movement of the droplets, brings down the probability of electrolysis despite the sharp corners present. The smooth motion of the droplet also enables the droplet driving system to automate the droplet operations under both ac and dc actuation.

3.3 Characterization of the Integrated Chip

A 1.5 µl droplet of electrolyte is dispensed onto the control electrode. Due to the problem of electrolysis under ac actuation on the SiN coated devices, a dc actuation potential is used to move the droplets. The droplet is transported towards the through hole with a dc actuation potential of 40 V. Figure 11 shows the cross section of the different test structures. Figure 11 (a) shows the device structure with 5% coverage of the through hole by the last electrode. While actuating the droplet over the last electrode of this device, it moves very slowly inside the through hole. This slow transportation can be attributed to the force being less than that required on the droplet at the side wall slope of the through hole. This could be because of a low coverage of the side wall slope with the control electrode, as the droplet experiences electromechanical force only where the control electrode is present. This geometry also requires multiple actuations over the last electrode to make the droplet fall inside the through hole. These

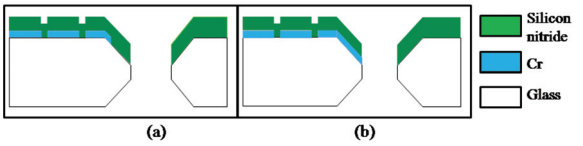

Fig. 11.Cross section view of structures with (a) 5% coverage and (b) 50% coverage of the through hole with the last electrode

multiple actuations eventually lead to electrolysis at the last electrode and damage the device permanently after delivering about five droplets inside the through hole.

Another test structure is fabricated by covering half of the through hole with the control electrode (Figure 11(b)). This 50% coverage of the through hole extends the metal layer of the control electrode to the sidewall slope of the through hole and provides the necessary force required for the transportation of the droplet into the microreactor in the bonded wafer below. This design does not require multiple actuations on the last electrode unlike that for the geometry shown in Figure 11(a) which increases the lifetime of the device. Figure 12 shows the top view of the sequential frames of transportation of the liquid droplets inside the through hole with the structure shown in Figure 11(b). Though this structure moves the droplet smoothly over the last electrode, the droplet does not enter the through hole completely and gets stuck in the neck of the through hole around the side slope as shown in the last frame of Figure 12. This is

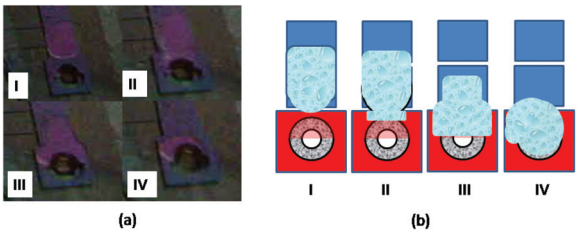

Fig. 12 Sequential frame showing transportation of the electrolyte on the integrated chip and its sticking inside the through hole of diameter 1.3 mm: (a) frames taken from a movie file (b) schematics corresponding to the frames

confirmed by the C-V measurement on the bonded microreactor which does not yield any change in capacitance with the voltage sweep. This problem occurs due to the small size of the through hole (1.3 mm diameter) which prevents escape of the air and hinders the delivery of the fluidic reagents to the microreactor below. The problem is solved by increasing the through hole diameter to 2.2 mm with a 50% electrode coverage fabricated with the same process flow described in Figure 5. Figure 13(a) shows the top view of the integrated device. For these devices, the electrolyte was successfully delivered to the microreactor in the bonded wafer below. The transported electrolyte goes into the through hole and fills the microreactor in the bonded silicon wafer below. This completes the electrical connection with the top contact being the gold electrode patterned along the sidewall slope of the through hole connected to the electrolyte of the EISCAP biosensor while the back contact is the

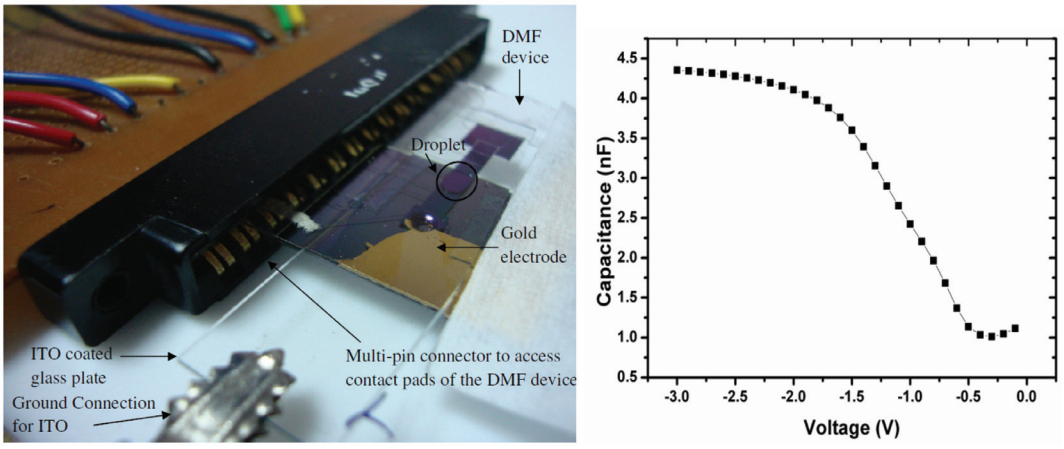

Fig. 13 a) Top view of the new integrated device and b) C-V curve measured on integrated EISCAP biosensor for electrolyte solution of pH4

ohmic contact to the silicon substrate. The C-V characteristics, measured using an Agilent E4980A LCR meter at 10 kHz with a 50 mV signal amplitude by sweeping the dc bias from -3 to 0 V in steps of 100 mV, is shown in Figure 13(b). The variation in the CV, as expected for typical EISCAPs [Veeramani *et al*, 2013], confirms the successful delivery of the electrolyte into the EISCAP microreactor via the through hole.

4. Conclusions

A basic DMF platform is fabricated with automated droplet operations on the DMF device using a PSoC and electromagnetic relay circuitries. Basic droplet operations like cutting, transporting, and dispensing on DI water are demonstrated under ac actuation. However, while transporting electrolytes, this results in electrolysis which damages the device permanently. It is observed that the use of a dc actuation potential can solve the problem of electrolysis, but charges the dielectric layer. Interdigitated electrode design is shown to mitigate this problem and to improve the device performance and reliability. The integration of an EISCAP microreactor with a DMF device is presented. For the integrated device, the dimension of the through hole in the DMF chip and its alignment with the last driving electrode is seen to play a major role in the successful and reliable delivery of the droplet to the bonded microreactor below. A DMF device with a through hole of 2.2 mm diameter and with 50% electrode coverage is shown to successfully deliver the droplet into the EISCAP microreactor. The presented integrated device accommodates the electrical sensing of the electrolyte inside the bonded microreactor as seen from the CV characteristics.

Acknowledgement

The authors would like to thank Dr. Aaron R Wheeler, Department of Chemistry, University of Toronto for sharing his experience in DMF. We also acknowledge the help of S. Mohanasundaram, C. Rajendran and R. Nagarajan of the Microelectronics and MEMS Laboratory, Electrical Engineering Department, IIT Madras for help with the experiments.

References

Abdelgawad M. and Wheeler A. R., 2009, The digital revolution: a new paradigm for microfluidics, Adv. Mater., 21(8), 920-925.

Chang Y. S., Lee G. B., Huang F. C., Chen Y. Y., Lin J. L., 2006, Integrated polymerase chain reaction chips utilizing digital microfluidics Biomed Microdevices, 8(3), 215-225 .

Chatterjee D., Hetayothin B., Wheeler A. R., King D. J. and Garrell R. L. 2006, Droplet-based microfluidics with nonaqueous solvents and solutions Lab Chip, 6, 199-206 .

Cho S. K., Moon H., and Kim C. –J., 2003, Creating, transporting, cutting, and merging liquid droplets by electrowetting- based actuation for digital microfluidic circuits, J. Microelectromech. S., 12(1), 70-80.

Fair R. B., 2007, Digital microfluidics: is a true lab-on-a-chip possible?, MicrofluidNanofluid, 3(3), 245-281.

Jones T B., 2005, An electromechanical interpretation of elecrowetting, J. Micromech. Microeng., 15(6), 1184-1187.

Mugele F. and Baret J-C., 2005, Electrowetting: from basics to applications, J. Phys.: Condens. Matter, 17(28), R705-R774.

Pollack M.G., Fair R.B. and Shenderov, A.D., 2000, Electrowetting-based actuation of liquid droplets for microfluidic applications, Appl. Phys. Lett., **77**(11), 1725-1726.

Pollack M. G., Shenderov, A. D. and Fair R. B., 2002, Electrowetting-based actuation of liquid droplets for integrated Microfluidics Lab Chip, 2, 96-101.

Veeramani M. S., Shyam P., Ratchagar N. P., Chadha A., Bhattacharya E., and Pavan S., 2013, A miniaturized pH sensor with an embedded counter electrode and a readout circuit, to appear in IEEE Sensors J. 2013, available on line doi: 10.1109/JSEN.2245032.

Paresh Kumar did his B.E. in electronics and communication engineering from MBM Engineering College, Jodhpur in 2007, and MS. (by Research) in electrical engineering from the Indian Institute of Technology

Madras, Chennai, India, in 2012. His M.S. thesis dealt with Digital Microfluidic (DMF) devices and their interfacing with biosensors. He spent six months at Prof. A. Wheeler's laboratory at the U. of Toronto with a fellowship from ISTP, Canada. Currently, he is a component design engineer with the Graphics Division, Intel Technology India Pvt. Ltd., Bangalore.

Enakshi Bhattacharya did her MSc (Physics) from IIT Bombay in 1980, PhD from TIFR Mumbai in 1985 and Post-doctoral work at the National Renewable Energy Laboratory (then SERI), USA from 1986-88. She was a faculty member in the Department of Physics, IIT Kanpur during 1988-91. Since 1991, she has been on the faculty of the Department of Electrical Engineering at IIT Madras and is currently a Professor. In 1999-2000 she was a Visiting Scientist at the Micromachined Products Division of Analog Devices, USA. She is interested in all forms of silicon: single crystal, poly, amorphous and porous and her current research areas are MEMS/NEMS and Biosensors.